

## **Effect of Elevated Temperature and Humidity on Fibers Based on 5-amino-2-(*p*-aminophenyl)**

### **benzimidazole (PBIA)**

**Amy Engelbrecht-Wiggans<sup>1,2</sup>, Thanh Nhi Hoang<sup>1,3</sup>, Viviana Bentley<sup>1,3</sup>, Ajay Krishnamurthy<sup>1,2</sup>, Lucas Kaplan<sup>1</sup>, and Amanda L. Forster<sup>1</sup>**

<sup>1</sup>Material Measurement Laboratory, National Institute of Standards and Technology, Gaithersburg, MD, USA

<sup>2</sup>Theiss Research, La Jolla, CA, USA

<sup>3</sup>Chemical and Biological Sciences Unit, Montgomery College, Germantown, MD, USA

Amy Engelbrecht-Wiggans

e-mail address: aee@nist.gov, aee52@cornell.edu

Telephone number: (301) 975-8580

ORCID: 0000-0002-5292-7970

Amanda L. Forster

e-mail address: amanda.forster@nist.gov

Telephone number: (301) 975-5632

ORCID: 0000-0001-7397-4429

Mailing address for both Corresponding Authors Amy and Amanda:

National Institute of Standards and Technology

Gaithersburg, MD 20899

mailstop 8102

### **Abstract**

Soft body armor is typically comprised of materials such as aramid. Recently, copolymer fibers based on the combination of 5-amino-2-(*p*-aminophenyl) benzimidazole (PBIA) and PPTA were introduced to the body armor marketplace. The long-term stability of these copolymer fibers have not been the subject of much research, however they may be sensitive to hydrolysis due to elevated humidity because they are condensation polymers. Efforts to evaluate the impact of environmental conditions on fiber strength is very important for the adoption of these materials in armor systems. Three PBIA-based fibers were selected for the study, and were aged at 25 °C, 75 % RH; 43 °C, 41 % RH; 55 °C, 60 % RH; and 70 °C, 76 % RH for up to 524 d.

Molecular spectroscopy, scanning electron microscopy, and single fiber tensile testing were performed to characterize changes in their chemical structure, tensile strength, and failure strain as a function of exposure time to different conditions. The fibers were all found to have some reduction in strength at high humidity conditions, with an approximately 14 % reduction for the copolymers and a 29 % reduction for the homopolymer. Molecular spectroscopy revealed some changes which suggest that hydrolysis of the benzimidazole ring is occurring at these elevated temperatures, possibly explaining the observed change in strength.

### **Keywords**

Aramid fibers; Environmental degradation; Strength; Mechanical Testing

### **1. Introduction**

Reducing the weight of body armor used for personal protection for law enforcement and military applications has consistently been a topic of significant interest [1]. Materials such as poly(*p*-phenylene terephthalamide) (PPTA), or aramid, as well as ultra-high molar mass polyethylene (UHMPE) have been commonly used to provide for ballistic protection [2]. To reduce the weight of armor capable of stopping a specific ballistic threat, alternative high strength fiber materials have been developed, such as aramid copolymer fibers. These fibers based on [5-amino-2-(*p*-aminophenyl)benzimidazole] (amidobenzimidazole, ABI), *p*-phenylenediamine (*p*-PDA), and terephthaloyl chloride, forming poly(*p*-phenylene-benzimidazole-terephthalamide-co-*p*-phenylene terephthalamide), which have been the focus of several patents [3-5]. Fiber mechanical properties such as ultimate tensile strength and strain to failure are critical for ballistic protection [6-8]. Frequently, strength is quantified using a twisted yarn test, where the mechanical strength of the yarn bundle is measured. However, this test requires a large amount of material and the relationship between yarn properties and single fiber properties is complex, depending on the twist angle, the number of fibers and the individual fiber properties [9-11]. However, disentangling single fibers from the yarn bundle for single fiber testing has previously been a challenge in studying these copolymer materials. Prior work by McDonough [12] used water to disentangle yarns before executing single fiber tensile testing. However, questions remained as to whether or not the fiber mechanical properties were changed by this water exposure. Recently, an acetone and methanol rinse has been shown to be successful at removing the coating and

allowing for single fiber disentanglement [13]. Washing with acetone and methanol instead of water allows for the differentiation of hydrolysis in the fibers due to the environmental exposure versus that induced by sample preparation.

When selecting conditions for a laboratory ageing study, the use environment must be considered. Laboratory ageing studies are designed to accelerate conditions expected in the real world, typically by using an elevated temperature, without introducing new mechanisms of degradation or ageing [14]. A simplified assumption that soft body armor in use is worn 40 hours a week, 50 weeks a year for 5 years gives 417 continuous days of ageing, at near body temperature. The exposure humidity must be carefully selected, because while the outside of the armor is likely to be damp from sweat, the armor carrier is designed to protect the ballistic material from both liquid moisture and ultra-violet light. Thus, a dark, noncondensing hydrothermal environment is typically selected for these studies [14–16].

Significant efforts [12, 17] have been focused on examining the long-term stability of polymeric fibers used in body armor, such as PPTA, by investigating detrimental changes in these mechanical properties after exposure to environmental conditions. For PPTA, Auerbach [18] performed an analysis of the chemical kinetics of aramid degradation. This work was performed in the context of predicting aramid and nylon parachute lifetimes, so in addition to temperature and humidity exposure, yarns were tightly knotted to mimic the folding within the parachutes. Auerbach modelled the degradation of aramid with an empirical second-order rate relationship. Two primary degradation mechanisms were found. At low humidity, a thermo-oxidative degradation mechanism dominates. At high humidity, Auerbach found that a “moisture-induced” mechanism dominated, presumably hydrolysis. Springer [19] also determined a functional relationship between degradation and failure time, where there were two distinct degradation phases.

In contrast to PPTA, the effect of environmental conditions on aramid copolymer fibers has not been the subject of much research [12, 15, 20]. The goal of this project is to examine the effect of elevated humidity and temperature on the mechanical properties of aramid copolymer fibers. In this study, we examine three different fibers, all of which are commercially produced materials based on poly 5-amino-2-(*p*-aminophenyl)benzimidazole, or PBIA. Information on how PBIA copolymers are prepared has been previously published [2, 20, 21]. One homopolymer of this chemical structure and two random copolymers

with different ratios of PBIA and PPTA linkages are studied herein [15]. These fibers are designated as Copolymer A, Copolymer B, and Homopolymer. Four different environmental conditions were chosen, and extractions made at various times up to 524 days.

## 2. Experimental

### 2.1. Materials and ageing conditions

Copolymer yarns were wound on smooth bobbins and aged in an environmental chamber at either 25 °C and 75 % relative humidity (RH), 43 °C and 41 % RH, 55 °C and 60 % RH, or 70 °C and 76 % RH. These particular ageing conditions were chosen based on a prior study of PPTA at three of these ageing conditions, allowing for comparison. The environmental chambers used provided control to  $\pm 1$  °C and  $\pm 5$  % RH. The extraction times varied for the different conditions and are given in Table 1.

**Table 1** Extraction times (in days) and environmental conditions for the ageing study

All materials			Copolymer A & B	Homopolymer
25 °C, 75 % RH	43 °C, 41 % RH	55 °C, 60 % RH	70 °C, 76 % RH	70 °C, 76 % RH
123	119	124	166	158
213	210	213	268	324
297	237	287	304	425
386	327	376		461
	399	449		
	428	524		
	478			

### 2.2. Single fiber disentangling

As previously mentioned, the PBIA fibers are covered with an organic coating that hinders single fiber separation. Fibers were aged as-received; however, the coating was removed after exposure and prior to extracting single fibers for mechanical testing. The coating removal procedure is described in detail in another publication [13]. After the coating is removed, single fibers can be disentangled from the yarn with minimal

damage, and prior work has shown that this procedure does not cause significant chemical changes to the material [13].

### **2.3. Tensile measurements**

Tensile testing was performed on disentangled single fibers using two different experimental setups, one using templates, with the test performed in a TA Instruments<sup>1</sup> RSA-G2, and the other directly gripping the fibers, in a Favimat single fiber load frame. A careful comparison between the two test methods is presented below.

The templated fibers were glued to a cardstock template with cyanoacrylate glue as described in [13] and in ASTM standards C1557 and D3822 [22, 23]. For the directly gripped specimens, the direct fiber grips were made of PMMA, as recommended by a prior effort [24], and superseded any need to mount the single fibers in a template. This reduced the amount of handling of the fibers, which can cause mechanical damage, and reduced the testing time approximately by an order of magnitude. Furthermore, the direct gripping setup allowed for determination of the average cross-sectional area for each fiber by using a vibroscope according to ASTM Standard D1577 [25]. In contrast, an average cross-sectional area for all fibers was used for the templated fibers. For both testing methods, a gauge length of 20 mm and a crosshead speed of 0.75 mm/min were used.

### **2.4. Molecular Spectroscopy**

Non-quantitative Fourier Transform Infrared (FTIR) Analysis was performed using a Bruker Vertex 80 Fourier Transform Infrared Spectrometer, equipped with a Smiths Detection Durascope Attenuated Total Reflectance (ATR) accessory. High purity nitrogen passed over a desiccant cartridge was used as the purge gas. Yarns were mounted on adhesive film fiber cards for analysis. Constant pressure on the yarns was applied using the force monitor on the Durascope. FTIR spectra were recorded at a resolution of 4 cm<sup>-1</sup> between 4000 cm<sup>-1</sup> and 800 cm<sup>-1</sup> and averaged over 128 scans. Three different locations on each yarn were analyzed. Standard uncertainties associated with this measurement are typically  $\pm 4$  cm<sup>-1</sup> in wavenumber and

---

<sup>1</sup> Certain commercial entities, equipment, or materials may be identified in this document in order to describe an experimental procedure or concept adequately. Such identification is not intended to imply recommendation or endorsement by the National Institute of Standards and Technology, nor is it intended to imply that the entities, materials, or equipment are necessarily the best available for the purpose.

$\pm 1$  % in peak intensity, thus using propagation of error, the uncertainty in intensity in the normalized curve is  $\pm 1.4$  %.

### **2.5. Scanning Electron Microscopy (SEM)**

Prior to electron imaging, the fibers were first mounted onto a stainless stub using a conductive carbon tape and then sputter coated with a thin coating (nominally 4 nm) of gold/palladium. SEM images were then acquired using an electron beam with a 2 kV electron-beam-voltage and 100 pA beam current. Magnifications ranging between 50 X and 3500 X were used to study the fiber surfaces.

### **2.6. Moisture Content Measurements**

Yarn segments of each fiber of interest were conditioned in humidity chambers at 25 °C and 75 % RH, 25 °C, 27 % RH for at least 10 days. Conditioned yarns were removed from the chambers and immediately weighed to determine an equilibrium moisture content for each condition. The conditioned yarns were then placed in an oven at 120 °C and allowed to dry for at least 48 h. The yarns were then placed in a desiccator to cool for at least 30 min. The cooled yarns were then weighed again to determine a dry weight. The difference between the two weights was taken as the moisture content. This experiment was repeated three times. For the yarns designated as representative of laboratory conditions, specimens were taken from the laboratory and weighed, then dried according to the procedures described above to determine the moisture content.

## **3. Results and Discussion**

### **3.1. Gripping method comparison**

Specimens of the same fiber type and ageing conditions were tested using both the template testing method and the direct fiber gripping method. All data associated with this work is archived through the National Institute of Standards and Technology (NIST) Public Data Repository [26]. Figure 1 is an overlay of stress-strain curves for directly-gripped and template-mounted unaged single fibers. To accurately compare directly-gripped and mounted specimens, all stresses calculated in Figures 1 and 2 use the average fiber diameter as measured for the directly-gripped specimens (fiber diameter histograms for directly-gripped fibers are provided in the Appendix). For the unaged copolymer fibers, the two gripping methods result in virtually identical stress-strain curves, as indicated by near total overlap. For the unaged homopolymer the overlap is less, and the variation of the directly-gripped fibers is less than that of the mounted fibers indicating that the

directly-gripped fibers show less variation in Young's modulus than the mounted fibers. For the unaged homopolymer fibers, Figure 1d compares the failure strength distribution for the two gripping methods, plotted on a Weibull plot. The two distributions are very similar, indicating that the failure strength for the unaged homopolymer is not significantly affected by the gripping method. The extended lower tail may be caused either by weakening of the fibers with handling or by using an average fiber diameter as the cross section for all fibers. Extended lower tails are less common with the direct-gripped fibers than with the mounted fibers, particularly when the actual average fiber diameter is considered [27]. Figure 1e compares the failure strain distributions for the two gripping methods for the unaged homopolymer fibers, plotted on a Weibull plot. From the 30<sup>th</sup> percentile and greater, the two distributions are nominally parallel to each other, implying a fixed offset between the two different gripping methods. It is unlikely that this offset is due to slip, as none of the characteristics of slippage [13] appear in the stress strain curves in Figure 1.

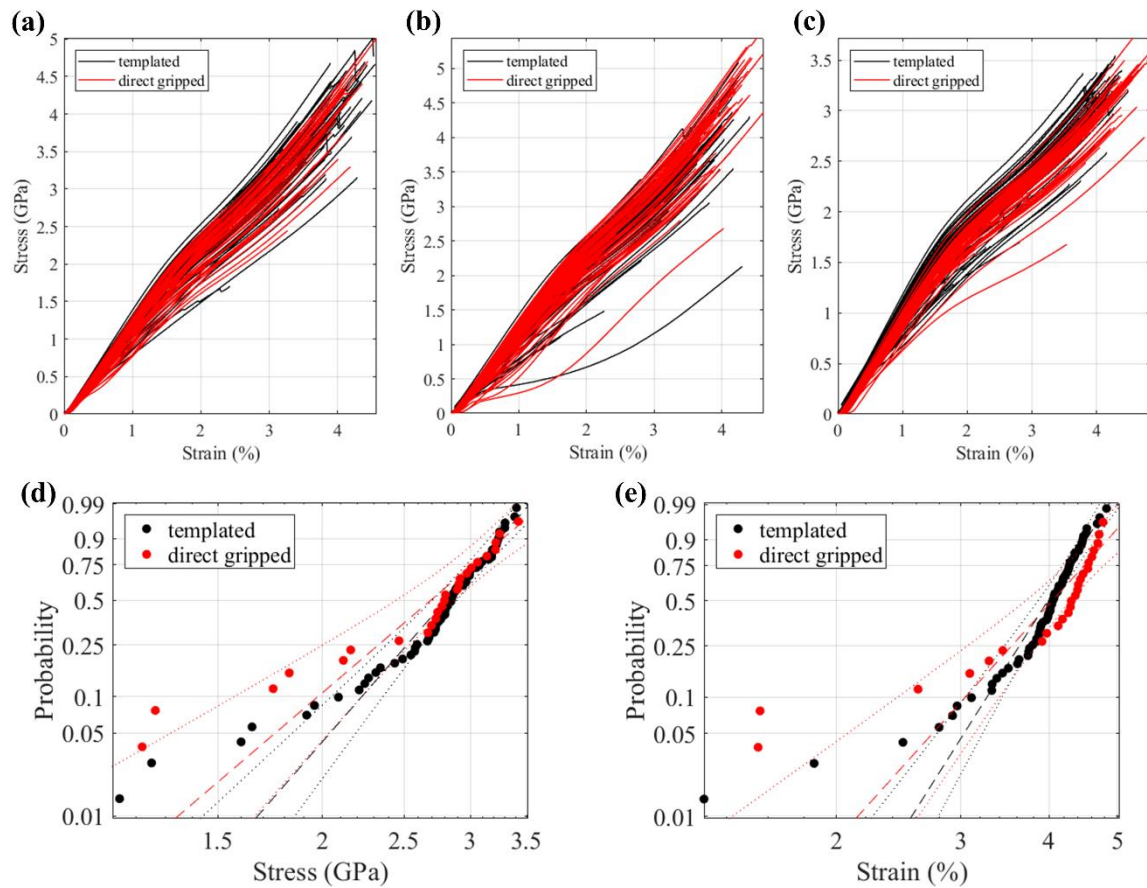


**Figure 1** Overlay of stress-strain curves for the mounted (black) and directly-gripped (red) specimens for a) copolymer A, b) copolymer B, and c) the homopolymer. Failure d) stress and e) strain distributions for the

mounted (black) and directly-gripped (red) homopolymer specimens, using an average diameter of 13.5  $\mu\text{m}$ . This diameter measurement is based on vibroscope measurements of 80 specimens. Dashed lines are the Maximum Likelihood Estimate (MLE) for the distribution, and dotted lines are the 95 % MLE confidence interval.

When the same comparison is performed for the aged fibers, however, the disagreement between the two methods is greater, as can be seen in Figure 2. Mounted specimens require more handling, so if the aged specimens are more susceptible to mechanical damage, the increased handling could cause earlier failures in templated specimens, as is observed in the two copolymers. Due to the difference in results shown above for the aged material, only data generated using the directly-gripped method will be presented below.

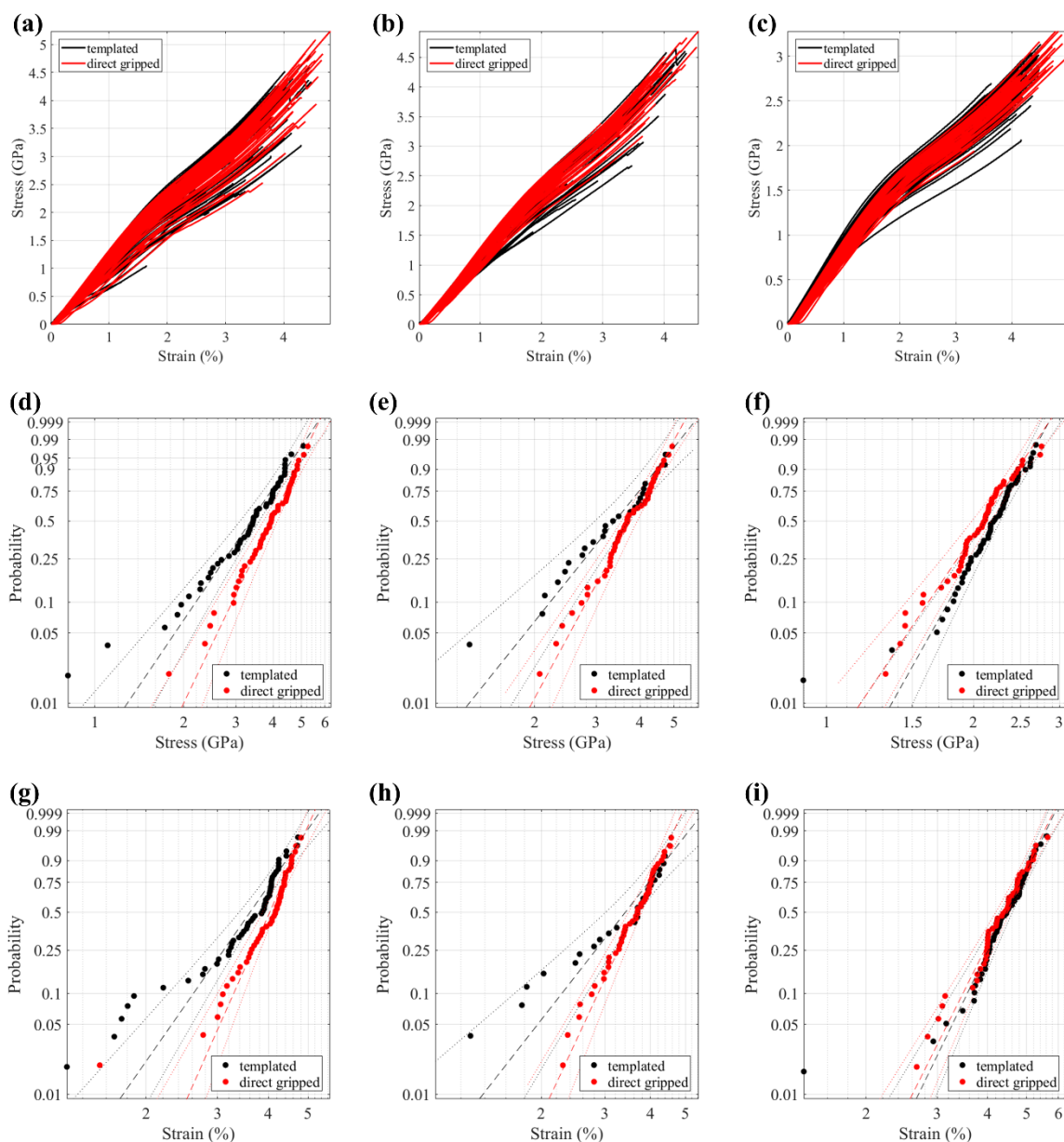


**Figure 2** Comparison between mounted (black) and directly-gripped (red) (a, d g) Copolymer A, aged 449 d at 55 °C and 60 % RH, (b, e, h) Copolymer B, aged 399 d at 43 °C and 41 % RH and (c, f, i) the homopolymer aged 376 d at 55 °C and 60 % RH, where (a, b, c) are overlays of the stress strain curves, (d, e, f) are the failure stress distributions using an average cross-sectional area, and (g, h, i) are the strain to failure distributions, also using an average cross-sectional area.

### 3.2. Mechanical Properties Determination

Tensile testing was performed on unaged and aged samples of the three materials, as described above.

Histograms of the fiber diameters are given in Figure A1. Three different statistics were considered for presentation: the average, the median, and the Weibull scale parameter. The average is the most common statistic; however, it is sensitive to outliers, and is less appropriate for a skewed distribution. The median has less sensitivity to outliers; however, the Weibull scale parameter was chosen as the main statistic since the failure stress, failure strain, and modulus are all approximately Weibull distributed [28]. Three different error bars were also considered: the standard deviation, the standard error, and a 95 % confidence interval. The standard deviation is most commonly used, however the distributions in question are so broad that using the standard deviation for error bars frequently hides any degradation. The standard error of the mean, i.e. the standard deviation divided by the square root of the number of specimens, and the 95 % confidence interval are both dependent on the number of specimens tested, such that if the number of specimens varies widely the error bars will also vary, giving a false implication that the underlying variability has also changed. For this dataset, the number of specimens is relatively similar for most ageing conditions. The 95 % confidence interval was chosen as for the strength values it gives a good indication of when the distributions differ.

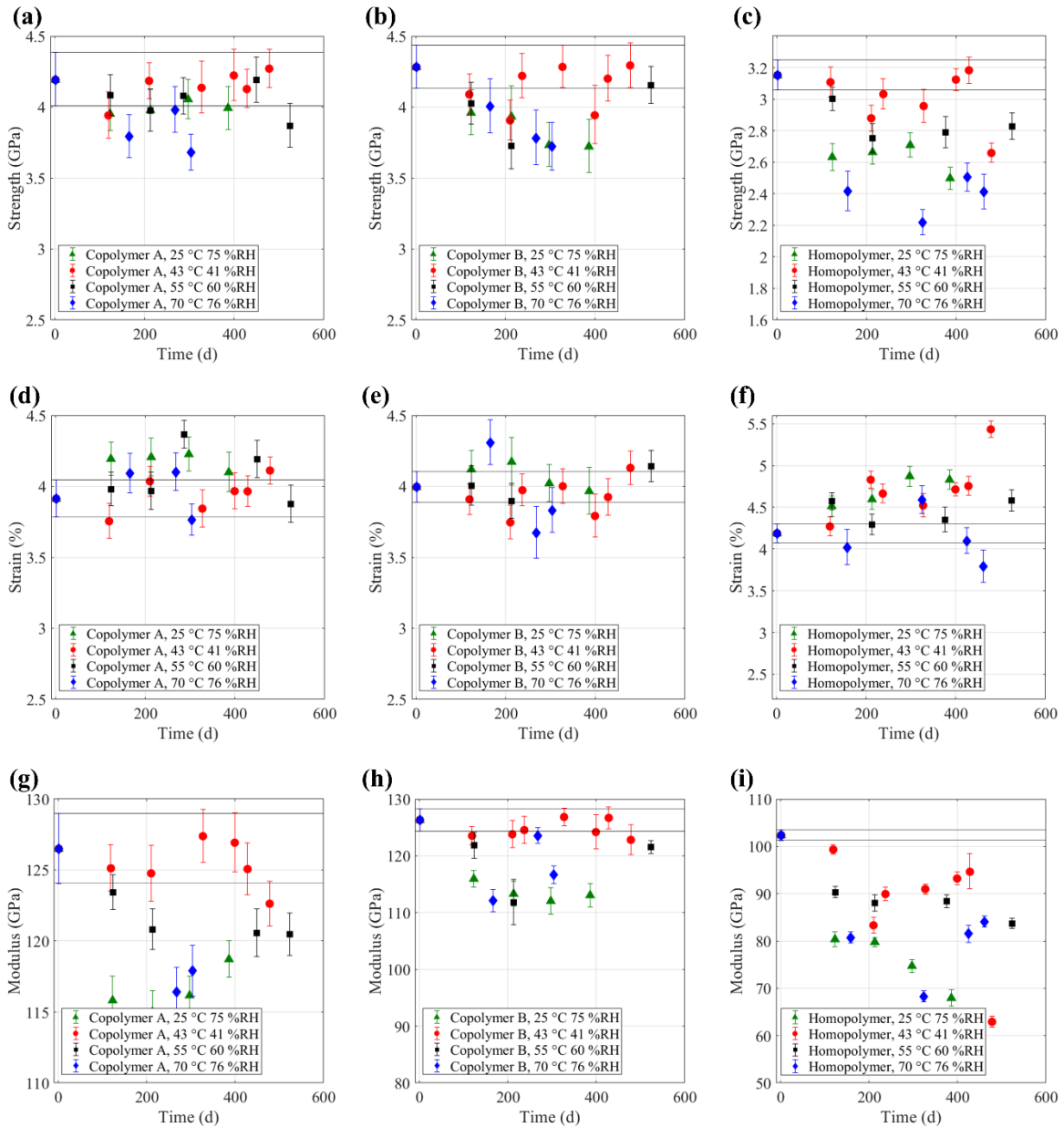


**Figure 3** Weibull scale parameter and 95 % confidence interval for Copolymer A, Copolymer B and Homopolymer (a, b, c) strength, (d, e, f) strain to failure and (g, h, i) elastic modulus, respectively. The solid horizontal lines represent the 95 % confidence intervals for the unaged samples.

Figure 3 shows the change in tensile strength, strain and Young's modulus as a function of exposure time for directly-gripped specimens of Copolymer A, Copolymer B, and the Homopolymer. Each datapoint is the maximum likelihood estimator (MLE) scale parameter of at least 50 specimens, and the error bars are 95 % MLE confidence intervals. The mean values with standard deviation error bars for the modulus are given for

comparison in Figure 4. Exact numbers of specimens, failure strengths, failure strains and moduli are given in the Appendix in Table A1, A2, A3 and A4 respectively. Solid black horizontal lines have been drawn on Figure 3 at the error bars for the unaged material.

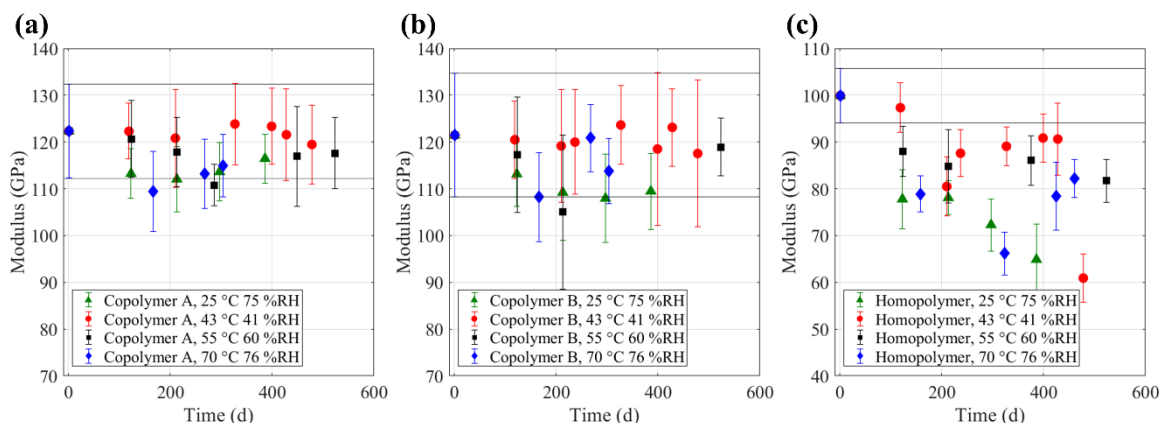


**Figure 4** Mean and standard deviation of the modulus, with horizontal solid lines at one standard deviation away from the mean, for a) Copolymer A, b) Copolymer B, and c) the homopolymer.

For these materials, tested at these conditions, the stress strain curves are not linear, but instead have a kink centered at around 2 % strain [9, 20, 29], potentially due to the low crystallinity of the fibers [13, 20, 21, 29–32]. It is hypothesized that, at less than 2 % strain, there is reorientation of the macromolecules, which upon unloading form structured blocks and new intermolecular bonds. Covalent bonds, in contrast, are only broken near failure [29, 33]. Due to this kink in the stress strain curves, the Young’s modulus is thus calculated from the initial linear region, between 0.16 % and 1.5 % strain. These values were chosen as the region with the highest linearity, after careful examination of the data. Below 0.16 % strain there are occasional initial loading effects, whereas the kink typically starts shortly after 1.5 % strain, particularly for the homopolymer. Theoretically, one would expect to observe monotonically decreasing trends for strength of fiber with ageing, however, the data presented below was experimentally-determined. Given the challenges in separating and testing single fibers, there is even more scatter associated with this data than would be expected in typical degradation studies which do not always show monotonic decreases [34]. Given the sparsity of data surrounding ageing in this material system, there is still value in investigating the ageing properties of these fibers.

For Copolymer A, any degradation in strength is minimal with exposure time (see Figure 3a), and only the 70 °C and 76 % RH data has no overlap of error bars. At 70 °C and 76 % RH, there is 12 % degradation in strength after 303 days (d). There is more scatter in the strain to failure data than in the other data, with little evidence of any long-term change. The modulus values appear to change slightly, ending at a value lower than that of the original modulus, which will be discussed further below. Figure 3b, for Copolymer B, indicates more degradation in the strength than was seen for Copolymer A. Only the 43 °C and 41 % RH data exhibits no change with ageing time. Similar ageing results are observed for the three other temperature/humidity conditions with respect to strength, with 13 % degradation in strength after 303 d at 70 °C and 76 % RH. Failure strains remain relatively constant for all ageing conditions; thus, the modulus is observed to degrade over time. The homopolymer results, shown in Figure 3c and Figure 3i, display greater strength and modulus change than the copolymers. For example, there was 24 % degradation in strength after 461 d at 70 °C and 76 % RH, and the 324 d datapoint at the same conditions exhibited 30 % strength degradation. The failure strain does not appear to be degrading significantly, and for the 43 °C and 41 % RH condition appears to increase, though this is not correlated with much degradation in the failure strength. The modulus of the homopolymer changes over time, with three different sets of data having significant (more than 30 %) degradation.

In comparison, the strength of PPTA twisted yarns, from two manufacturers, were found to have degraded 7 % and 13 % after 280 d of exposure to 70 °C and 76 % RH [35]. At 303 d Copolymer A degraded 11 %, and Copolymer B degraded 13 %, while the Homopolymer degraded 29 % after 324 d. Thus, the copolymer fibers have similar degradation levels to PPTA fiber.

For both Copolymer B and the Homopolymer, the low temperature and high humidity condition (25 °C and 75 % RH) had similar levels of degradation to the 70 °C and 76 % RH condition. This indicates a sensitivity to the moisture content, which was noted before for the homopolymer in [15], but will be discussed further below.

The effect of ageing on the modulus is perhaps overstated in Figure 3, because of the narrow error bars. To investigate this, Figure 4 presents the mean and standard deviation of the modulus, while Figure 5 shows overlays of aged vs unaged stress-strain curves. Figure 4 gives the impression of no significant change in

modulus for either of the copolymers, while in contrast the homopolymer's modulus still shows degradation. Figure 5 overlays stress-strain curves for unaged and aged material at the longest ageing time, allowing a visual comparison of how the stress-strain curves change with ageing. The 70 °C, 76 % RH condition was selected for this comparison because it is the harshest ageing condition. For Copolymer A there are two unaged specimens with a higher modulus than the aged material, and one with a lower. This places the initial linear portion of the aged material directly on top of the unaged, however the upper portion of the curves may be shifted down when compared to the unaged. For Copolymer B the aged material is again bracketed by the unaged, both for the first linear portion as well as when the strain is greater than 2 %. Both of these appear to have a slight downwards shift in the stress-strain curves after 2 % strain, and a potential shift for smaller strain values. For the homopolymer, Figure 5c, there is a clear downwards shift at all strain values, and the modulus, strength and failure strain can all be seen to have decreased.

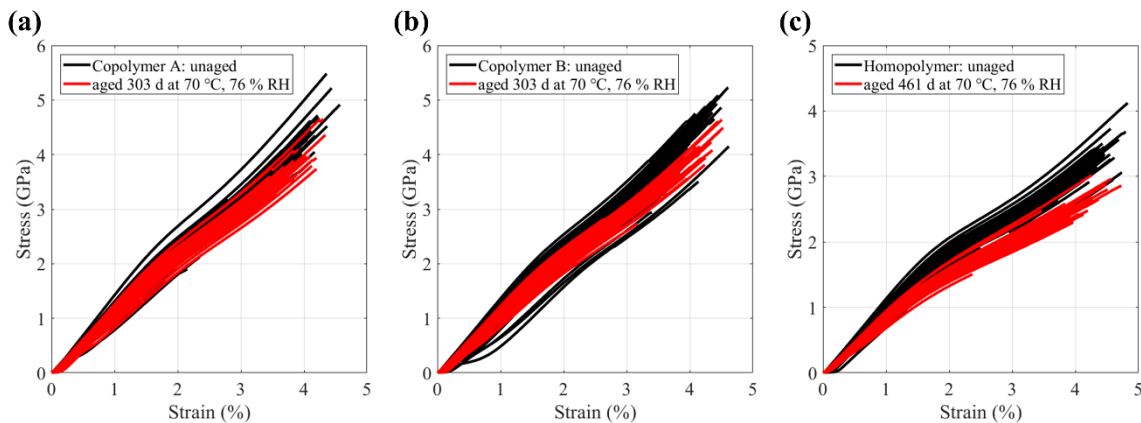


**Figure 5** Example overlays of data from aged and unaged data specimens for of a) copolymer A, b) copolymer B, and c) the homopolymer, using measured cross-sectional areas.

There are several factors that could cause a decrease in modulus with ageing. If the molecular chains become less stiff, then this would result in an overall softening of the material. A loss of orientation could also cause a change in stiffness. In comparison to PPTA fibers, the more amorphous nature of these degraded fibers may lead to a load sharing behavior that could result in a decrease in modulus. The effects of a loss of stiffness and a change in orientation can be modeled with the Eindhoven Glassy Model [36], which was developed for highly oriented amorphous polyethylene. While past studies have shown a weaker dependence of modulus on orientation [29], from the molecular spectroscopy results presented below (Section 3.4, Figure 10 and Figure

A5) there is reason to believe that the benzimidazole ring may open as a result of ageing, which would decrease the molecular stiffness.

Attempts were made to fit the Auerbach [18] and Springer [19] degradation models to this strength data; however, the amount of degradation seen here is so minimal, and the failure distributions are so broad that a meaningful fit could not be obtained. Furthermore, there is no clear trend in the Weibull shape parameters for the strength, strain or modulus for all three materials.

### **3.3. Ageing and Failure Morphology**

SEM microscopy was used to obtain a visual comparison of unaged and degraded fibers. Copolymer A fibers appear to be relatively unchanged due to ageing, which supports the mechanical property data. Homopolymer fibers appear to become rougher with ageing with the appearance of longitudinal grooves. Micrographs for these two fibers are found in the Appendix.

As shown in Section 3.2, the mechanical properties of the Copolymer B fibers aged at the 55 °C, 60 % RH condition were reduced at ageing times of 213 d and 449 d, but then were observed to return to slightly below the initial tensile strength after 524 d. Initially, it was assumed that this was an erroneous result, so 20 new fibers from this extraction were washed and tested. However, these additional measurements confirmed that the increased tensile strength was correct. Only small quantities remained of the fibers aged to 213 days and 449 days, so additional tensile testing on these samples was not possible. To investigate the reduced tensile strength observed in these fibers, SEM was performed. A figure combining the SEM micrographs with ageing time and average tensile strength is given in Figure 6. The micrographs from several different fibers showed that there were clear physical differences in the fibers aged to 213 days and 449 days as compared to the unaged fibers, or the fibers aged to 524 days. The fibers with the lower tensile strength exhibited significant surface roughness, grooves, and overall mechanical damage. In particular, the second micrograph for 213 days shows obvious circumferential banding, indicative of mechanical damage.

In contrast, the fibers aged to 524 days appeared smooth and undamaged and were very close to the unaged fibers in appearance. For comparison, Copolymer B fibers aged for 303 days at 70 °C, 76 % RH, which exhibited a reduction in mechanical properties, were also imaged (Figure 6, top center) and did not exhibit a

significant change in physical appearance as compared to the unaged fibers. Based on this analysis, we surmise that the fibers aged at 213 days and 449 days were mechanically damaged, either before ageing or during the process of being prepared for tensile testing. Mechanical damage has been shown to be detrimental to the strength of high performance fibers [37], [38], and we attribute the reduction in strength at these conditions to microscopic damage incurred to the extracted fibers during washing and specimen preparation as opposed to hydrolysis due to ageing. This damage was only detected when microscopy was performed on untested fibers from the same extraction, after tensile testing was completed.

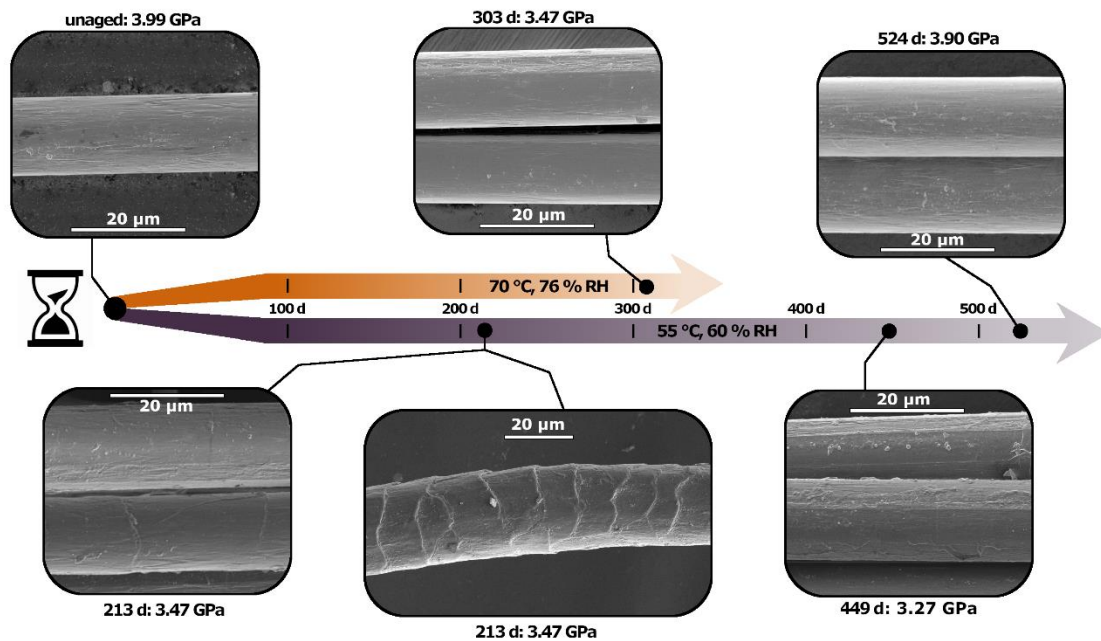


**Figure 6** Timeline combining the SEM micrographs with average tensile strength for Copolymer B aged at 55 °C, 60 % RH (purple) and 70 °C, 76 % RH (orange).

For specimens that have a higher than average failure load, failure involves a large amount of fibrillation that can extend for over 6 mm, as depicted in Figure 7. In contrast, the damaged area on weak fibers is much more localized, and typically is less than 1mm, as shown in Figure 8. This observation was consistent across all material types and is analogous to the failure behavior previously noted for pure PPTA fibers. In PPTA there are three failure modes: a) pointed break, b) fibrillated break, and c) kink band break, which originates from mechanical damage [10]. The presumption is that the weak fibers are failing due to a local flaw, and when flaws are not present, we see a long fibrillation length associated with the fiber failure. Generally, the

fibrillation appears longer in the copolymer fibers than has been observed in PPTA [27]. This indicates that more slippage and splitting of the fibrillar structure occurs in these fibers than in PPTA, which could be attributed to the generally amorphous morphology of these copolymer materials [13], [20], [29], [30], [32], [39].

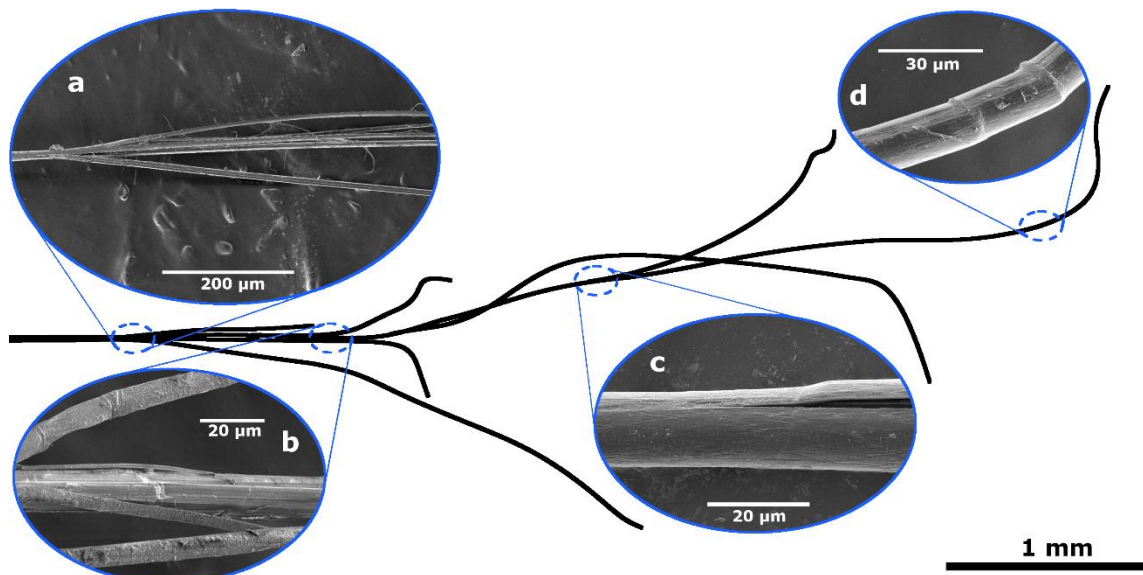


**Figure 7** Schematic of characteristic failure for a strong fiber, with typical SEM images of a) fiber fibrillating into multiple strands, b) fractured fiber surface, c) crack initiation, and d) kink bands from bending. Note that not all images are representative of the same failed fiber.

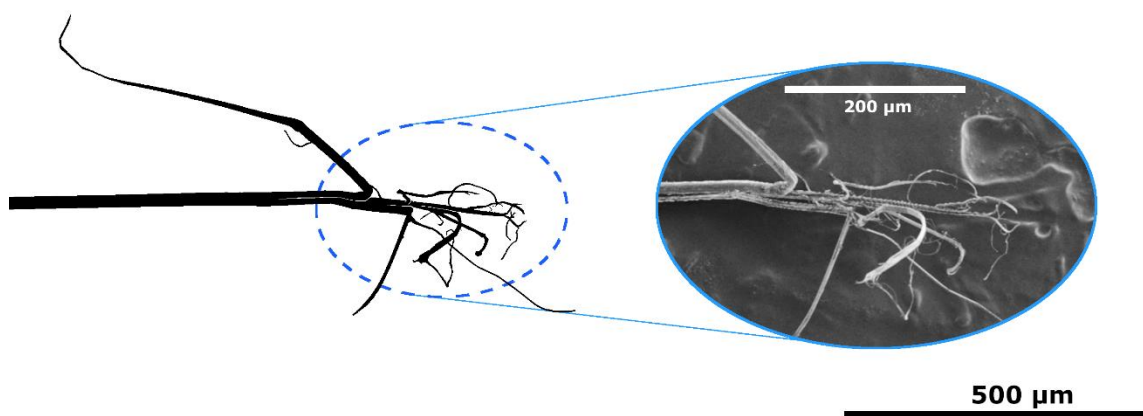


**Figure 8** Schematic of characteristic failure for weak fibers.

### 3.4. Chemical Changes due to Ageing

Molecular spectroscopy was used to characterize chemical changes in the three fibers after ageing to determine what, if any, chemical changes occurred in the polymer. Two likely reactions that could occur in

response to the hydrolytic environment are opening of the benzimidazole ring [40] and chain scission [16], [18], [19] at an amide bond. Schematics for these two potential reactions are presented for the fibers in Figure 9.

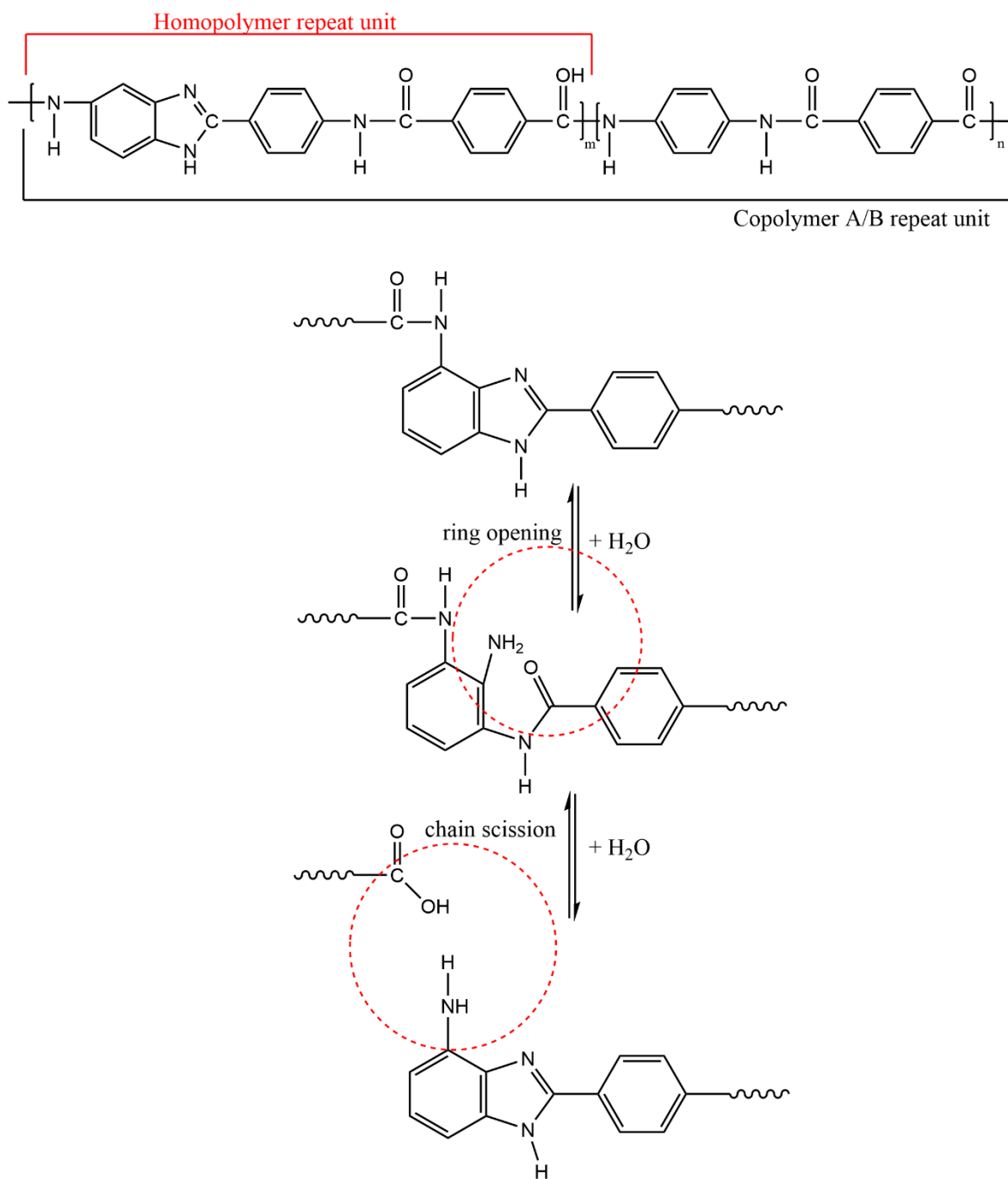
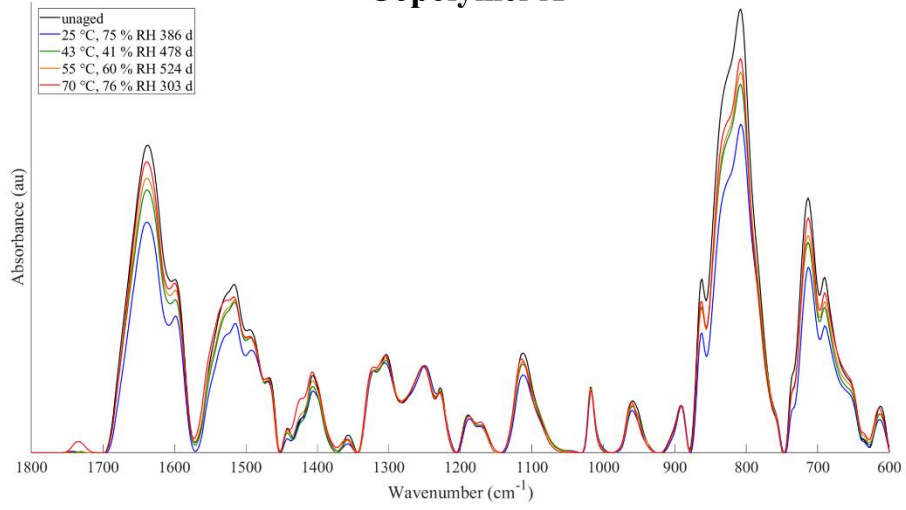


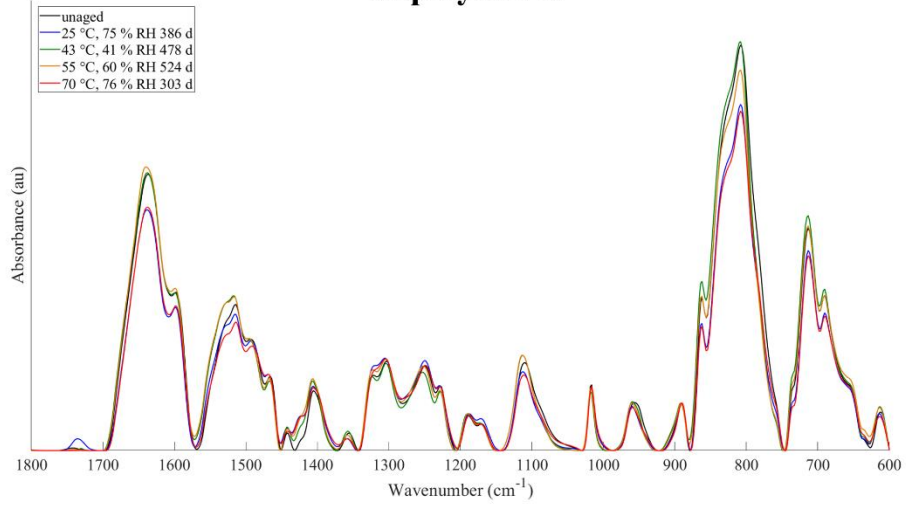
**Figure 9** Schematic of repeat unit for the copolymers and homopolymer (top) and proposed mechanisms for hydrolytic ring opening and chain scission in the fibers (bottom) [42].

ATR-FTIR is not a quantitative method, so only general observations of changes in peak features can be determined from analysis of this data. The ATR-FTIR spectra from  $1800\text{ cm}^{-1}$  to  $600\text{ cm}^{-1}$  are presented in Figure 10 with a broader set of spectra ( $4000\text{ cm}^{-1}$  to  $500\text{ cm}^{-1}$ ) given in Figure A5. All spectra shown are the average of three measurements and were intensity normalized with a peak at  $890\text{ cm}^{-1}$ , which is attributed to CH out of plane stretch [41]. This peak was selected for normalization because the expected hydrolysis mechanism would not change the CH bonds corresponding to the out of plane CH stretching vibrations of the aromatic ring observed in this region. The normalization is intended only to assist in making comparisons between the spectra. Copolymer A showed the smallest change in tensile properties of all the materials, and similarly, an analysis from molecular spectroscopy shows only slight changes in the chemical structure of the fiber, as shown in Figure 10 (top). Peaks associated with the benzimidazole ring ( $1491\text{ cm}^{-1}$ ,  $1470\text{ cm}^{-1}$ ,  $1443\text{ cm}^{-1}$ ,  $1188\text{ cm}^{-1}$ , and  $1111\text{ cm}^{-1}$ ) [41] are unchanged by ageing at  $25\text{ }^{\circ}\text{C}$ ,  $43\text{ }^{\circ}\text{C}$ , and  $55\text{ }^{\circ}\text{C}$ . At the  $70\text{ }^{\circ}\text{C}$  exposure temperature, where hydrolysis would be expected to proceed at the fastest rate [18], the formation of a shoulder peak associated with the benzimidazole ring around  $1432\text{ cm}^{-1}$  is evident. In addition, there is some evidence of the formation of a new carboxylic acid group ( $1734\text{ cm}^{-1}$ ) in the specimen aged at  $70\text{ }^{\circ}\text{C}$  [41]. These results could implicate either chain scission or ring opening of Copolymer A when aged at  $70\text{ }^{\circ}\text{C}$  for 301 days, although these changes do not appear to have much impact on the tensile strength, strain to failure, or modulus of this fiber.

### Copolymer A



### Copolymer B



### Homopolymer

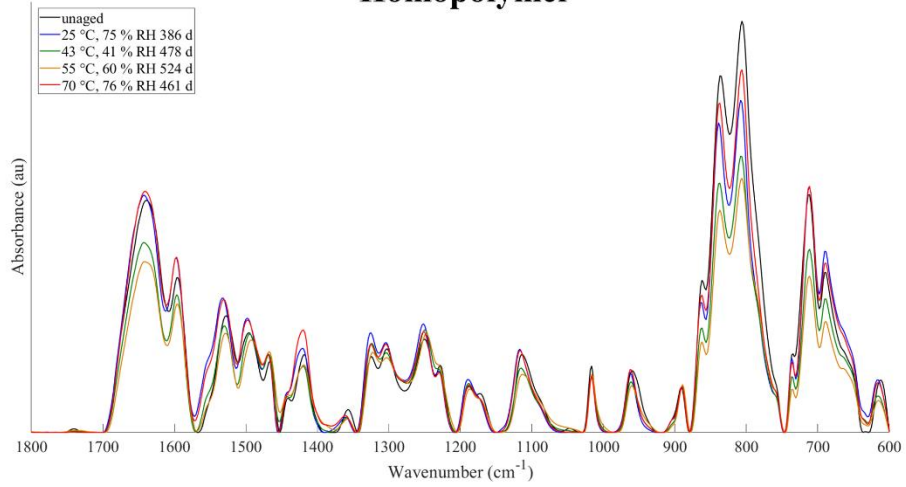


**Figure 10** ATR-FTIR spectrograms for Copolymer A (top), Copolymer B (middle) and Homopolymer (bottom) showing results for the longest aged sample at each set of conditions.

For Copolymer B, the largest change in tensile strength and modulus was for the highest humidity ageing conditions of 25 °C, 75 % RH and 70 °C, 76 % RH. Some similar changes in the FTIR spectra to those observed in Copolymer A are detected, notably the formation of a new peak around 1736 cm<sup>-1</sup> for the specimen aged at 25° C, 75 % RH. This peak could also be attributed to the creation of a carboxylic acid group [42] due to chain scission. Changes in the shape of the benzimidazole peak at 1423 cm<sup>-1</sup> are also observed for all ageing conditions, and these changes were most pronounced for the 25 °C, 75 % RH, 55 °C, 60 % RH, and 70 °C, 76 % RH conditions, whereas in Copolymer A this change was only observed in the 70 °C, 76 % RH condition, which could be indicative of ring opening. This observation could potentially explain the more pronounced loss in tensile strength and changes in modulus with ageing that were observed for Copolymer B.

The homopolymer also showed the most significant change in tensile properties for the highest humidity ageing conditions of 25 °C, 75% RH and 70 °C, 76 % RH, and exhibited the largest changes in tensile strength with ageing overall among the three fibers studied. Some similar changes consistent with chain scission to those observed in Copolymers A and B were detected. The changes in the shape of the benzimidazole peak that were observed in the other copolymers were not observed, perhaps indicating that ring opening is not a significant mechanism for this material. Overall, the molecular spectroscopy results for Homopolymer are inconclusive, and do not provide enough information to determine with certainty which hydrolysis mechanism is responsible for the changes in mechanical properties with ageing that were observed for this material.

### **3.5. Tensile strength sensitivity to moisture**

The tensile strength of aramids is very sensitive to the moisture content in the material [43], [44]. An experiment was performed, according to the procedure outlined above, to investigate the moisture content and its effects for these materials at three different conditions: laboratory conditions, 25 °C and 27 % RH, and 25 °C and 75 % RH. Laboratory conditions were monitored at least every 30 minutes over the course of a month with 17,700 observations. The mean temperature and relative humidity were 21.6 °C and 50.9 % RH with

standard deviations of  $\pm 0.5$  °C and  $\pm 1.4$  % RH. The 27 % RH condition was chosen as in PPTA; it results in 3 % by mass moisture content, which is the same as the conditions 43 °C and 41 % RH, 55 °C and 60 % RH, and 70 °C and 76 % RH, as seen in Figure A1 in the Appendix. In PPTA yarns, 25 °C and 75 % RH results in approximately 7.1 % moisture content by mass. For the three different conditions of laboratory (21.6 °C and 50.9 % RH), 25 °C and 27 % RH, and 25 °C and 75 % RH, the measured moisture content is presented in Figure 11 as well as Table A8 in the Appendix. Previous studies have compared the moisture content in copolymer PBIA, homopolymer PBIA and PPTA. The copolymers were found to have less moisture sorption than the homopolymer [32], but more than PPTA [20, 45]. This is consistent with the results at laboratory conditions and at 25 °C and 27 % RH, however at 25 °C and 75 % RH none of the copolymers have sorbed as much moisture as the PPTA yarns.

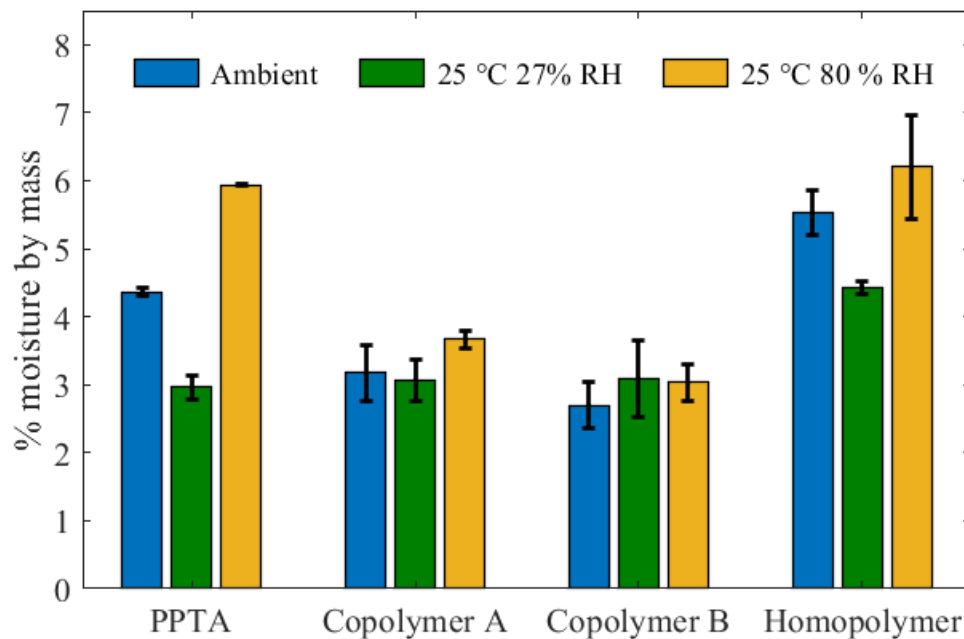


**Figure 11** Average moisture content with standard deviations error bars calculated from three replicates

Tensile testing was performed on the 25 °C and 27 % RH specimens, and Figure 12 compares these results with those from the unaged, laboratory acclimated specimens (21.6 °C and 50.9 % RH). Of these three materials, the homopolymer exhibits the greatest change with conditioning, which corresponds with what is observed in Figure 3 for the 25 °C and 75 % RH data. In that data, the first datapoint is for specimens

conditioned at 25 °C and 75 % RH for 123 d, and the homopolymer results show a large drop in strength and an increase in strain, both consistent with the changes seen in Figure 12 for the homopolymer. For Copolymer B there is no significant changes in Figure 12, particularly for the failure strain, and correspondingly Figure 3e has the smallest change in failure strain for the 123 days at 25 °C and 75 % RH sample of all three materials. For Copolymer A the laboratory conditioned sample has a lower failure strain and may be slightly weaker than the 25 °C and 27 % RH sample. Figure 3d for Copolymer A does show an increase in failure strain for the 123 d 25 °C and 27 % RH sample. These observations may be attributed to sorbed moisture acting as a plasticizer in the polymer [46].

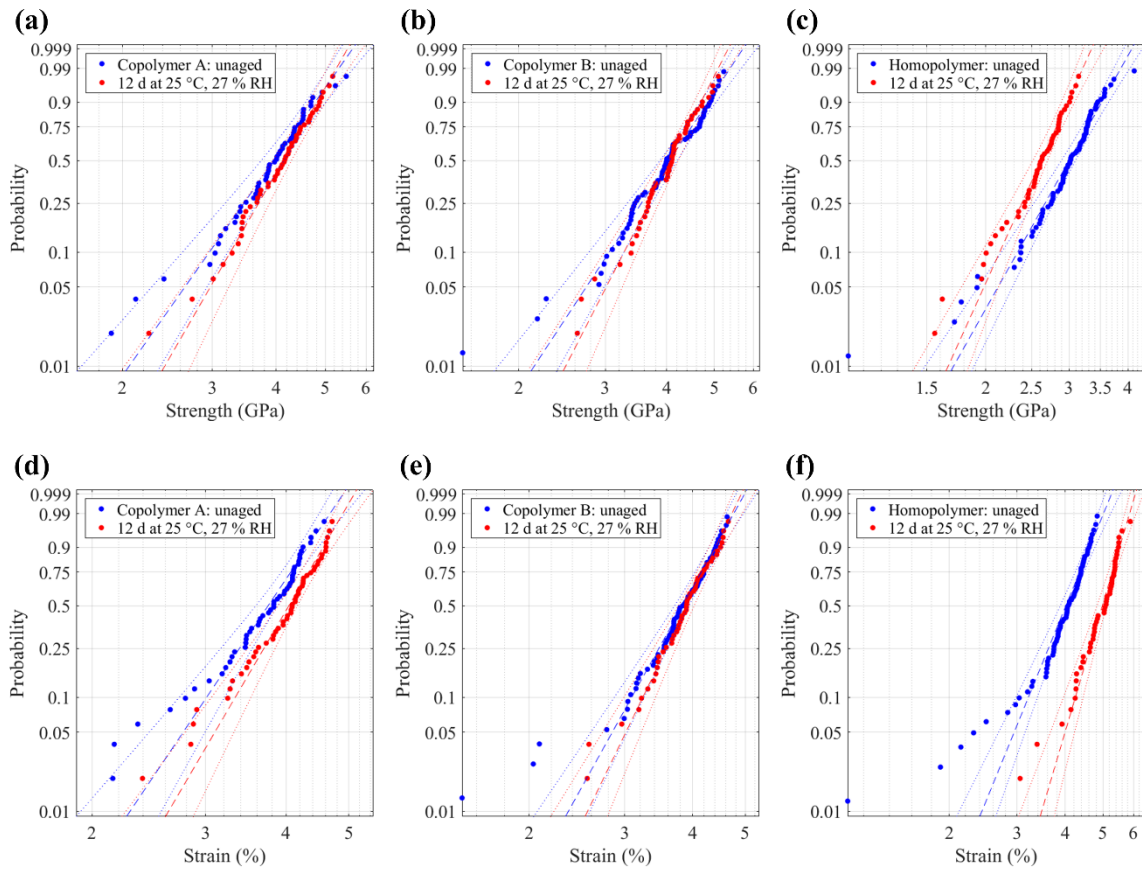


**Figure 12** Comparison of unaged material and material in conditioned at 25 °C and 27 % RH for 12 days: failure stress distributions for a) copolymer A, b) copolymer B, and c) the homopolymer, and failure strain distributions for d) copolymer A, e) copolymer B, and f) the homopolymer, using measured cross-sectional areas.

#### 4. Conclusions

This study has investigated the effect of elevated temperature and relative humidity on the mechanical properties of fibers based on 5-amino-2-(p-aminophenyl) benzimidazole. After exposure, it was determined that there is some change in mechanical properties in all three fibers investigated, however this change is less than 29 %. The two copolymer fibers demonstrated a smaller change (less than 14 %) in mechanical properties than the homopolymer. This indicates a similar sensitivity to moisture as PPTA for the copolymer fibers. The homopolymer, in contrast, had more than twice the degradation of the PPTA and copolymer fibers at 70 °C and 76 % RH. Molecular spectroscopy revealed some chemical changes which could be attributed to hydrolysis in the fibers but did not provide enough information to propose a clear mechanism of degradation for these materials. An attempt was made to apply models typically used for ageing in PPTA to this material, but as the fibers were generally robust and the failure distributions broad, there was insufficient degradation to make this analysis meaningful. Generally, considering that most soft body armor is warranted for 5 years of service, and the armor is used at conditions of body temperature and humidity, the exposure conditions in this study likely surpassed the amount of hydrolytic exposure expected during field use. The fiber failure morphology was found to be similar to that of PPTA, however on a longer scale. Higher strength fibers were found to have a fibrillated failure zone on the order of 6 mm, while weaker fibers typically had a more localized failure with less than 1 mm of fibrilization. Future work includes applying theoretical models of highly oriented glassy polymer models to describe the structure property relationships with ageing.

### **Acknowledgements**

The authors would like to acknowledge Gale Holmes for assistance with Favimat single fiber measurements, Faraz Ahmed Burni for assistance with the moisture measurements, and Vivian Yu and Shefei Jiang for assistance in preparing single fiber templates.

### **Conflicts of Interest**

The authors declare that they have no conflicts of interest in presenting this work. Funding for Engelbrecht-Wiggans was provided under cooperative agreement NIST 70NANB17H337. Funding for Krishnamurthy was provided under cooperative agreement NIST 70NANB18H226.

### **References**

- [1] A. Joseph, A. Wiley, R. Orr, B. Schram, and J. J. Dawes, "The impact of load carriage on measures of

- power and agility in tactical occupations: A critical review,” *Int. J. Environ. Res. Public Health*, vol. 15, no. 1, 2018.
- [2] J. W. S. Hearle, Ed., *High-performance fibres*. Boca Raton, FL: CRC Press, 2001.
- [3] R. E. T. P. De Vos, J. E. Surquin, and E. J. Marlieke, “United States Patent 8,362,192 B2 Large Scale Process for Polymerization of DAPBI-Containing Polyaramid,” 2013.
- [4] K. S. Lee, “United States Patent 8,716,434 Aramid Copolymer,” 2014.
- [5] F. K. Mallon, “United States Patent 8,716,430 Aramid Copolymer,” 2014.
- [6] P. M. Cunniff, “Dimensionless Parameters for Optimization of Textile-Based Armor Systems,” in *18th International Symposium on Ballistics*, 1999, pp. 1302–1310.
- [7] P. M. Cunniff, J. W. Song, and J. E. Ward, “Investigation of High Performance Fibers for Ballistic Impact Resistance Potential,” in *International SAMPE Technical Conference Series*, 1989, vol. 21, pp. 840–851.
- [8] M. Cheng, W. Chen, and T. Weerasooriya, “Mechanical Properties of Kevlar® KM2 Single Fiber,” *J. Eng. Mater. Technol.*, vol. 127, no. 2, p. 197, 2005.
- [9] J. W. S. Hearle, *High Performance Fibers*. Cambridge: Woodhead Publishing, 2001.
- [10] H. H. Yang, *Kevlar Aramid Fiber*. New York, NY: John Wiley and Sons, 1993.
- [11] P. K. Porwal, I. J. Beyerlein, and S. L. Phoenix, “Statistical strength of a twisted fiber bundle: an extension of daniels equal-load-sharing parallel bundle theory,” *J. Mech. Mater. Struct.*, vol. 1, no. 8, pp. 1425–1447, Dec. 2006.
- [12] W. G. McDonough *et al.*, “Testing and analyses of copolymer fibers based on 5-amino-2-(p-aminophenyl)-benzimidazole,” *Fibers Polym.*, vol. 16, no. 9, pp. 1836–1852, 2015.
- [13] A. L. Forster, V. Rodriguez Cardenas, A. Krishnamurthy, Z. Tsinas, A. Engelbrecht-Wiggans, and N. Gonzalez, “Disentangling High Strength Copolymer Aramid Fibers to Enable the Determination of Their Mechanical Properties,” *J. Vis. Exp.*, no. 139, p. e58124, Sep. 2018.
- [14] J. Chin, A. Forster, C. Clerici, L. Sung, M. Oudina, and K. Rice, “Temperature and humidity aging of poly(p-phenylene-2,6-benzobisoxazole) fibers: Chemical and physical characterization,” *Polym. Degrad. Stab.*, vol. 92, no. 7, pp. 1234–1246, 2007.

- [15] G. H. R. Messin, K. D. Rice, M. A. Riley, S. S. Watson, J. R. Sieber, and A. L. Forster, "Effect of moisture on copolymer fibers based on 5-amino-2-(p-aminophenyl)- benzimidazole," *Polym. Degrad. Stab.*, vol. 96, no. 10, pp. 1847–1857, 2011.
- [16] A. L. Forster *et al.*, "Hydrolytic stability of polybenzobisoxazole and polyterephthalamide body armor," *Polym. Degrad. Stab.*, vol. 96, no. 2, pp. 247–254, 2011.
- [17] G. A. Holmes, J.-H. Kim, D. L. Ho, and W. G. McDonough, "The Role of Folding in the Degradation of Ballistic Fibers," *Polym. Compos.*, vol. 31, pp. 879–886, 2010.
- [18] I. Auerbach, "Kinetics for the tensile strength degradation of Nylon and Kevlar yarns," *J. Appl. Polym. Sci.*, vol. 37, no. 8, pp. 2213–2227, 1989.
- [19] H. Springer, A. A. B. U. Obaid, A. B. Prabawa, and G. Hinrichsen, "Influence of Hydrolytic and Chemical Treatment on the Mechanical Properties of Aramid and Copolyaramid Fibers," *Text. Res. J.*, vol. 68, no. 8, pp. 588–594, 1998.
- [20] K. E. Perepelkin, "High-strength, high-modulus fibres made from linear polymers: Principles of fabrication, structure, properties, and use," *Fibre Chem.*, 2010.
- [21] L. Luo *et al.*, "The introduction of asymmetric heterocyclic units into poly(p-phenylene terephthalamide) and its effect on microstructure, interactions and properties," *J. Mater. Sci.*, vol. 53, no. 18, pp. 13291–13303, 2018.
- [22] "ASTM C1557-14 Standard Test Method for Tensile Strength and Young' s Modulus of Fibers," pp. 1–10, 2014.
- [23] "ASTM D3822/D3822M-14 Standard Test Method for Tensile Properties of Single Textile Fibers," *ASTM Int. U.S.A.*, no. June, pp. 1–10, 2015.
- [24] J. H. Kim *et al.*, "Effect of fiber gripping method on the single fiber tensile test: II. Comparison of fiber gripping materials and loading rates," *J. Mater. Sci.*, vol. 50, no. 5, pp. 2049–2060, 2015.
- [25] "ASTM D1577-07 (2018) Standard Test Methods for Linear Density of Textile Fibers," *ASTM Int. U.S.A.*, 2018.
- [26] A. Engelbrecht-Wiggans and A. L. Forster, "Data Publication: Aged and unaged PBIA-based copolymer testing for soft body armor applications." NIST Public Data Repository, Gaithersburg,

MD, 2019.

- [27] J. H. Kim *et al.*, “Effects of fiber gripping methods on the single fiber tensile test: I. Non-parametric statistical analysis,” *J. Mater. Sci.*, vol. 48, no. 10, pp. 3623–3637, 2013.
- [28] C. Croarkin and P. Tobias, “NIST/SEMATECH e-handbook of statistical methods,” *Retrieved January*, 2014.
- [29] V. A. Kvaratskheliya, “Ph.D. Dissertation: A study of microstructural changes in synthetic fibers resulting from mechanical deformations,” De Montfort University, 2001.
- [30] K. E. Perepelkin, N. N. Machalaba, and V. A. Kvaratskheliya, “Properties of Armos para-aramid fibres in conditions of use. Comparison with other para-aramids,” *Fibre Chem.*, vol. 33, no. 2, pp. 105–114, 2001.
- [31] A. A. Levchenko, E. M. Antipov, N. A. Plate’, and M. Stamm, “Comparative analysis of structure and temperature behaviour of two copolyamides - Regular KEVLAR and statistical ARMOS,” *Macromol. Symp.*, vol. 146, pp. 145–151, 1999.
- [32] N. N. Machalaba, N. N. Kuryleva, L. V. Okhlobystina, P. A. Matytsyn, and I. A. Andriyuk, “Tver’ fibres of the Armos type: Manufacture and properties,” *Fibre Chem.*, vol. 32, no. 5, pp. 319–324, 2000.
- [33] E. S. Tsobkallo, O. I. Nachinkin, and V. A. Kvartskheliya, “Effect of preliminary loading on the deformation and strength properties of high-strength fibres,” *Fibre Chem.*, vol. 30, no. 3, pp. 168–171, 1998.
- [34] J. V. Deshpande and R. . P. . Suresh, “Non-Monotonic Ageing,” *Scand. J. Stat.*, vol. 17, no. 3, pp. 257–262, 1990.
- [35] K. D. Rice, A. E. Engelbrecht-Wiggans, E. Guigues, and A. L. Forster, “Evaluation of Degradation Models for High Strength p-Aramid Fibres Used in Body Armour,” in *Proceedings of the Personal Armour Systems Symposium*, 2018.
- [36] D. J. A. Senden, J. A. W. Van Dommelen, and L. E. Govaert, “Strain hardening and its relation to Bauschinger effects in oriented polymers,” *J. Polym. Sci. Part B Polym. Phys.*, 2010.
- [37] G. A. Holmes, J.-H. Kim, D. L. Ho, and W. G. McDonough, “The Role of Folding in the Degradation

- of Ballistic Fibers,” *Polym. Compos.*, vol. in press, 2009.
- [38] H. Kobayashi *et al.*, “The effect of folding on the internal structure of ballistic fibers,” in *International SAMPE Technical Conference*, 2011.
- [39] A. A. Levchenko, E. M. Antipov, N. A. Plate, and M. Stamm, “Comparative analysis of structure and temperature behaviour of two copolyamides - Regular KEVLAR and statistical ARMOS,” *Macromol. Symp.*, vol. 146, pp. 145–151, 1999.
- [40] P. Liu, M. Mullins, T. Bremner, J. A. Browne, and H. J. Sue, “Hygrothermal behavior of polybenzimidazole,” *Polymer (Guildf)*, 2016.
- [41] A. L. Forster, “Study of acid generation from copolymer fibers based on 5-amino-2-(*p*-aminophenyl)-benzimidazole,” *NISTIR 7592*, 2009.
- [42] R. M. Silverstein, G. C. Bassler, and T. C. Morrill, *Spectrometric Identification of Organic Compounds*, 5th ed. New York: John Wiley and Sons, 1991.
- [43] J. Z. Wang, D. A. Dillard, and T. C. Ward, “Temperature and stress effects in the creep of aramid fibers under transient moisture conditions and discussions on the mechanisms,” *J. Polym. Sci. Part B Polym. Phys.*, vol. 30, no. 12, pp. 1391–1400, 1992.
- [44] D. A. Mooney and J. M. D. MacElroy, “Differential water sorption studies on Kevlar 49 and as-polymerised poly (*p*-phenylene terephthalamide): Adsorption and desorption isotherms,” *Chem. Eng. Sci.*, vol. 59, no. 11, pp. 2159–2170, 2004.
- [45] V. Y. Lakunin, M. V. Shablygin, G. B. Sklyarova, and L. V. Tkacheva, “Assortment and properties of aramid fibres manufactured by Kamenskvolokno Co.,” *Fibre Chem.*, vol. 42, no. 3, pp. 143–151, 2010.
- [46] S. Rebouillat, M. Escoubes, R. Gauthier, and A. Vigier, “Characterization of KEVLAR fibers using selected probes,” *J. Appl. Polym. Sci.*, vol. 58, no. 8, pp. 1305–1315, 1995.

## Appendix

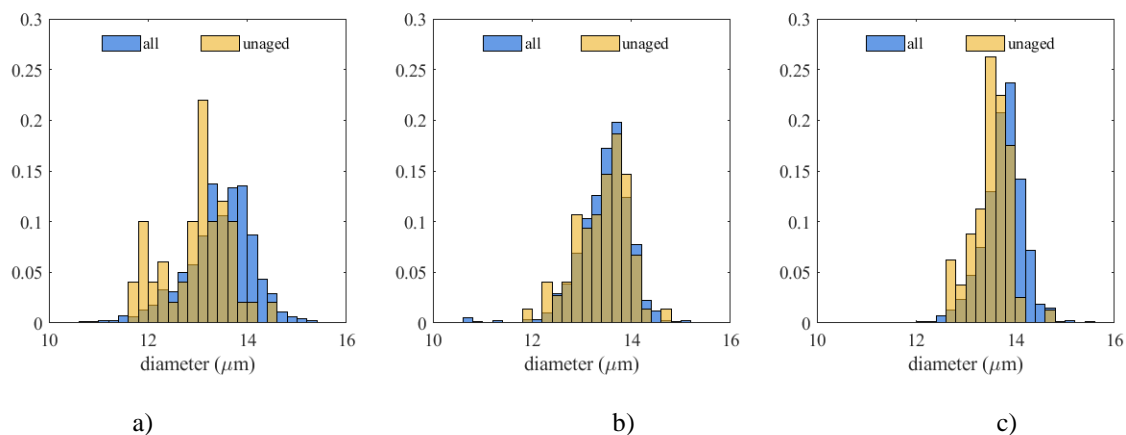


**Figure A1** Fiber diameter histograms for a) Copolymer A, b) Copolymer B, c) Homopolymer

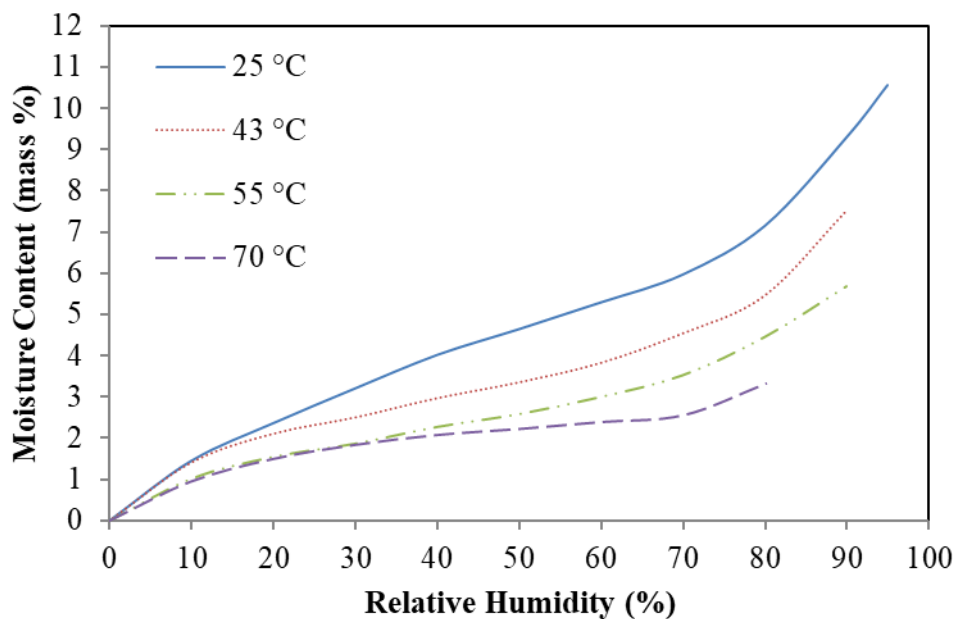
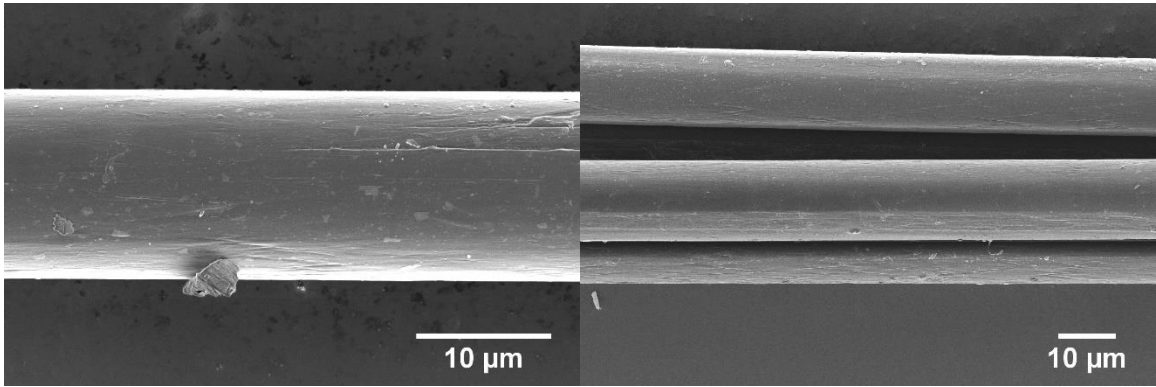


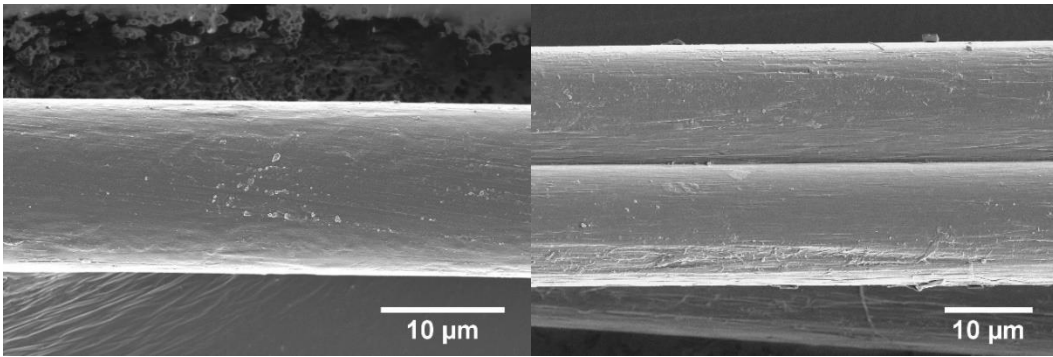
**Figure A2** Moisture content by mass of PPTA yarns as a function of the relative humidity at the temperatures 25 °C, 43 °C, 55 °C and 70 °C.



a)

b)

**Figure A3** Copolymer A SEM micrograph of a) unaged and b) aged fibers



a)

b)

**Figure A4** Homopolymer SEM micrograph of a) unaged and b) aged fibers

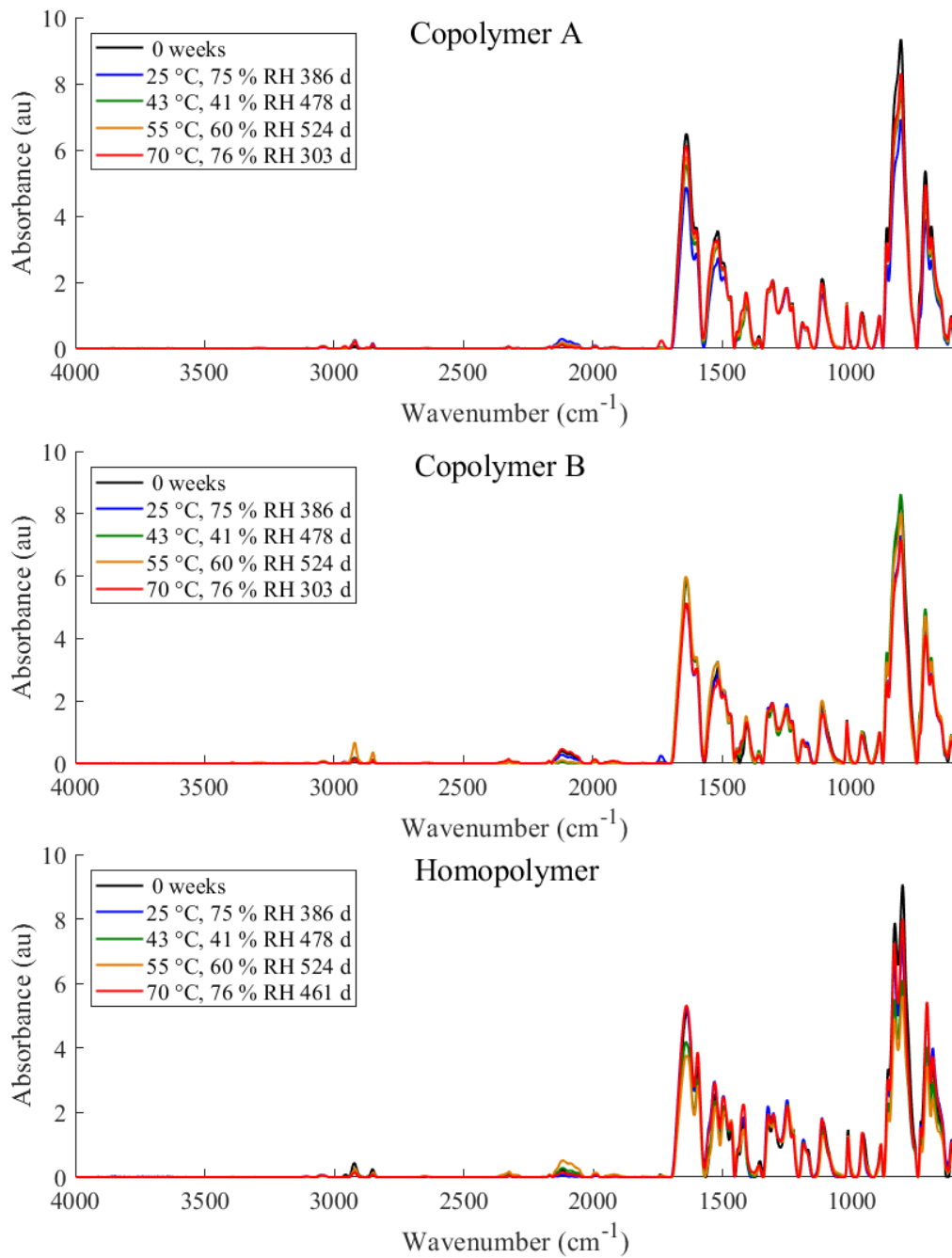


**Figure A5** ATR-FTIR spectrograms for Copolymer A (top), Copolymer B (middle) and Homopolymer (bottom) showing results for the longest aged sample at each set of conditions.

**Table A1** Number of directly-gripped tensile specimens at each ageing condition

conditions	N/A	25 °C, 75 % RH				43 °C, 41 % RH						
days aged	0	123	213	297	386	119	210	237	327	399	428	478

Copolymer A	50	50	50	50	50	50	50		50	50	50	50
Copolymer B	75	50	50	50	50	50	50	50	50	50	50	50
Homopolymer	80	50	49	50	50	50	50	50	50	50	50	50

conditions	55 °C, 60 % RH						70 °C, 76 % RH						
days aged	124	213	287	376	449	524	158	166	324	268	303	425	461
Copolymer A	50	50	50		50	50		50		50	50		
Copolymer B	50	100				70		50		50	50		
Homopolymer	50	49		50		50	49		50			50	50

**Table A2** Maximum likelihood estimated Weibull strength scale parameter of directly-gripped specimens with shape parameter in parentheses, all scale parameters in GPa, and the numbers of specimens given in Table A1

conditions	N/A	25 °C, 75 % RH					43 °C, 41 % RH						
days aged	0	123	213	297	386	119	210	237	327	399	428	478	
Copolymer A	4.19 (6.5)	3.95 (9.6)	3.98 (7.7)	4.05 (8.4)	3.99 (7.7)	3.94 (7.0)	4.18 (9.7)		4.14 (6.6)	4.22 (6.8)	4.13 (8.9)	4.27 (9.2)	
Copolymer B	4.28 (6.7)	3.96 (7.4)	3.93 (5.4)	3.73 (7.0)	3.72 (5.8)	4.09 (8.5)	3.91 (8.1)	4.22 (7.8)	4.28 (8.3)	3.98 (6.0)	4.20 (7.6)	4.29 (7.8)	
Homopolymer	3.15 (7.5)	2.63 (8.9)	2.66 (10.2)	2.71 (10.3)	2.50 (10.3)	3.11 (9.5)	2.88 (10.2)	3.03 (9.3)	2.96 (8.4)	3.12 (13.2)	3.18 (10.9)	2.66 (12.7)	

conditions	55 °C, 60 % RH						70 °C, 76 % RH						
days aged	124	213	287	376	449	524	158	166	324	268	303	425	461
Copolymer A	4.08 (8.4)	3.96 (7.6)	4.08 (9.3)		4.19 (7.6)	3.87 (7.4)		3.79 (7.3)		3.98 (7.2)	3.68 (8.5)		
Copolymer B	4.02 (7.9)	3.73 (6.5)				4.16 (7.8)		4.00 (6.1)		3.78 (5.7)	3.72 (6.5)		
Homopolymer	2.99 (11.1)	2.75 (8.8)		2.79 (8.3)		2.83 (9.9)	2.42 (5.6)		2.22 (8.0)			2.50 (8.1)	2.41 (6.4)

**Table A3** Maximum likelihood estimated Weibull strain scale parameter of directly-gripped specimens with shape parameter in parentheses, all scale parameters in %, and the numbers of specimens given in Table A1

conditions	N/A	25 °C, 75 % RH					43 °C, 41 % RH						
days aged	0	123	213	297	386	119	210	237	327	399	428	478	
Copolymer A	3.91 (8.6)	4.19 (10.4)	4.20 (9.3)	4.23 (10.1)	4.10 (8.6)	3.75 (9.0)	4.04 (11.1)		3.84 (8.5)	3.97 (9.0)	3.96 (10.6)	4.11 (12.8)	
Copolymer B	4.00 (8.7)	4.12 (9.2)	4.17 (7.2)	4.02 (8.9)	3.97 (7.0)	3.91 (10.6)	3.75 (9.2)	3.97 (10.3)	4.00 (9.5)	3.82 (7.9)	3.92 (8.8)	4.13 (10.1)	
Homopolymer	4.19 (8.4)	4.51 (10.8)	4.59 (11.3)	4.87 (11.7)	4.83 (11.9)	4.27 (11.0)	4.83 (13.4)	4.66 (12.0)	4.52 (9.5)	4.71 (17.4)	4.75 (12.0)	5.43 (15.6)	

conditions	55 °C, 60 % RH						70 °C, 76 % RH						
days aged	124	213	287	376	449	524	158	166	324	268	303	425	461
Copolymer A	3.98 (9.8)	3.96 (8.8)	4.37 (13.1)		4.19 (9.3)	3.88 (8.6)		4.09 (8.6)		4.10 (8.9)	3.76 (10.1)		
Copolymer B	4.00 (8.5)	3.90 (9.4)				4.14 (9.2)		4.31 (8.0)		3.67 (5.8)	3.83 (7.0)		
	4.56	4.29		4.35		4.58	4.01		4.59			4.10	3.79

Homopolymer	(12.8)	(10.1)		(8.6)		(10.2)	(5.5)		(8.0)			(7.7)	(5.7)
-------------	--------	--------	--	-------	--	--------	-------	--	-------	--	--	-------	-------

**Table A4** Maximum likelihood estimated Weibull modulus scale parameter of directly-gripped specimens with shape parameter in parentheses, all scale parameters in GPa, and the numbers of specimens given in Table A1

conditions	N/A	25 °C, 75 % RH				43 °C, 41 % RH						
days aged	0	123	213	297	386	119	210	237	327	399	428	478
Copolymer A	126 (15)	116 (20)	115 (22)	116 (25)	119 (27)	125 (22)	125 (18)		127 (20)	127 (18)	125 (20)	123 (22)
Copolymer B	126 (15)	116 (24)	113 (15)	112 (14)	113 (16)	124 (22)	124 (15)	125 (15)	127 (24)	124 (12)	127 (19)	123 (13)
Homopolymer	102 (21)	80 (15)	80 (24)	75 (16)	68 (11)	99 (29)	83 (15)	90 (19)	91 (25)	93 (20)	95 (8)	63 (16)

conditions	55 °C, 60 % RH						70 °C, 76 % RH						
days aged	124	213	287	376	449	524	158	166	324	268	303	425	461
Copolymer A	123 (28)	121 (24)	113 (28)		121 (20)	120 (23)		113 (19)		116 (19)	118 (19)		
Copolymer B	122 (15)	112 (8)				122 (26)		112 (16)		124 (26)	117 (22)		
Homopolymer	90 (21)	88 (15)		88 (19)		84 (22)	81 (20)		68 (17)			82 (13)	84 (21)

**Table A5** Average failure strength of directly-gripped specimens at each ageing condition, with standard deviations in parentheses, all strengths are in GPa, and the numbers of specimens given in Table A1

conditions	N/A	25 °C, 75 % RH				43 °C, 41 % RH						
days aged	0	123	213	297	386	119	210	237	327	399	428	478
Copolymer A	3.91 (0.72)	3.75 (0.49)	3.73 (0.62)	3.82 (0.60)	3.75 (0.60)	3.70 (0.55)	3.97 (0.50)		3.85 (0.71)	3.94 (0.70)	3.90 (0.57)	4.05 (0.50)
Copolymer B	3.99 (0.73)	3.71 (0.59)	3.62 (0.81)	3.49 (0.57)	3.44 (0.72)	3.86 (0.57)	3.68 (0.54)	3.96 (0.64)	4.04 (0.60)	3.70 (0.69)	3.94 (0.69)	4.03 (0.73)
Homopolymer	2.96 (0.49)	2.49 (0.32)	2.54 (0.27)	2.57 (0.32)	2.38 (0.26)	2.95 (0.39)	2.75 (0.32)	2.88 (0.37)	2.79 (0.39)	3.01 (0.27)	3.03 (0.39)	2.55 (0.26)

conditions	55 °C, 60 % RH						70 °C, 76 % RH						
days aged	124	213	287	376	449	524	158	166	324	268	303	425	461
Copolymer A	3.84 (0.60)	3.71 (0.63)	3.87 (0.49)		3.92 (0.69)	3.63 (0.60)		3.55 (0.61)		3.73 (0.61)	3.49 (0.44)		
Copolymer B	3.78 (0.60)	3.47 (0.65)				3.90 (0.61)		3.72 (0.72)		3.49 (0.73)	3.47 (0.62)		

Homopolymer	2.85 (0.34)	2.61 (0.34)		2.63 (0.37)		2.68 (0.36)	2.24 (0.45)		2.09 (0.30)			2.35 (0.37)	2.24 (0.42)
-------------	----------------	----------------	--	----------------	--	----------------	----------------	--	----------------	--	--	----------------	----------------

**Table A6** Average failure strain of directly gripped specimens at each ageing condition, with standard deviations in parentheses, all strains are in %, and the numbers of specimens given in Table A1

conditions	N/A	25 °C, 75 % RH					43 °C, 41 % RH						
days aged	0	123	213	297	386	119	210	237	327	399	428	478	
Copolymer A	3.69 (0.58)	3.99 (0.47)	3.98 (0.58)	4.01 (0.56)	3.86 (0.61)	3.56 (0.46)	3.86 (0.41)		3.62 (0.57)	3.75 (0.56)	3.77 (0.50)	3.95 (0.38)	
Copolymer B	3.77 (0.58)	3.91 (0.51)	3.89 (0.69)	3.80 (0.53)	3.70 (0.68)	3.72 (0.49)	3.55 (0.47)	3.77 (0.52)	3.79 (0.54)	3.59 (0.56)	3.70 (0.60)	3.93 (0.53)	
Homopolymer	3.95 (0.67)	4.30 (0.50)	4.39 (0.46)	4.65 (0.55)	4.63 (0.44)	4.06 (0.51)	4.64 (0.46)	4.46 (0.52)	4.28 (0.57)	4.56 (0.36)	4.53 (0.59)	5.25 (0.45)	

conditions	55 °C, 60 % RH						70 °C, 76 % RH						
days aged	124	213	287	376	449	524	158	166	324	268	303	425	461
Copolymer A	3.77 (0.52)	3.74 (0.58)	4.19 (0.42)		3.96 (0.60)	3.66 (0.57)		3.86 (0.58)		3.88 (0.57)	3.58 (0.42)		
Copolymer B	3.78 (0.54)	3.69 (0.50)				3.92 (0.56)		4.05 (0.65)		3.39 (0.74)	3.58 (0.63)		
Homopolymer	4.37 (0.48)	4.08 (0.52)		4.10 (0.59)		4.34 (0.62)	3.69 (0.83)		4.32 (0.65)			3.83 (0.69)	3.49 (0.77)

**Table A7** Average Young's modulus of directly-gripped specimens at each ageing condition, with standard deviations in parentheses, all moduli are in GPa, and the numbers of specimens given in Table A1

conditions	N/A	25 °C, 75 % RH					43 °C, 41 % RH						
days aged	0	123	213	297	386	119	210	237	327	399	428	478	
Copolymer A	122 (10)	113 (5)	112 (7)	114 (6)	116 (5)	122 (6)	121 (10)		124 (9)	123 (8)	122 (10)	119 (8)	
Copolymer B	121 (13)	113 (7)	109 (10)	108 (9)	109 (8)	120 (8)	119 (12)	120 (11)	124 (8)	119 (16)	123 (8)	118 (16)	
Homopolymer	99.9 (5.8)	77.8 (6.3)	78.1 (3.6)	72.3 (5.6)	64.9 (7.5)	97.3 (5.3)	80.5 (6.3)	87.6 (5.0)	89.1 (4.1)	90.9 (5.1)	90.6 (7.7)	60.9 (5.2)	

conditions	55 °C, 60 % RH						70 °C, 76 % RH						
days aged	124	213	287	376	449	524	158	166	324	268	303	425	461
Copolymer A	121 (8)	118 (7)	111 (4)		117 (11)	118 (8)		109 (9)		113 (7)	115 (7)		
Copolymer B	117 (12)	105 (16)				119 (6)		108 (9)		121 (7)	114 (7)		
Homopolymer	88.0	84.8		86.1		81.7	78.9		66.2			78.4	82.2

Homopolymer	(5.4)	(7.8)		(5.3)		(4.6)	(3.8)		(4.6)		(7.2)	(4.0)
-------------	-------	-------	--	-------	--	-------	-------	--	-------	--	-------	-------

**Table A8** Estimated average moisture contents, measured in % mass, with the standard deviation from three trials in parentheses

	Laboratory (% mass)	25 °C, 27 % RH (% mass)	25 °C, 75 % RH (% mass)
PPTA	4.36 (0.06)	2.96 (0.17)	5.94 (0.02)
Copolymer A	3.17 (0.40)	3.07 (0.30)	3.67 (0.33)
Copolymer B	2.70 (0.34)	3.09 (0.56)	3.03 (0.26)
Homopolymer	5.53 (0.33)	4.43 (0.10)	6.20 (0.77)